



3-1-8

GENERAL RULE OF STRONG-MOTION ARRAY LAYOUT FOR SOURCE STUDY

Masahiro IIDA, Takashi MIYATAKE, and Kunihiko SHIMAZAKI

Earthquake Research Institute, University of Tokyo,
Bunkyo-ku, Tokyo, Japan

SUMMARY

The first attempt to investigate the effects of strong-motion array layout for source inversion is done by estimating the accuracy of the inversion solution. Our source inversion method developed based on the Wolberg's prediction analysis is available for this purpose. Preliminary studies which consist of three parts, i.e., systematic analysis to reveal the effects of fault-array parameters, determination of optimum array geometry, and application of our method to existing networks have led us to conclude that the preferable array involves both the near-source stations and stations encircling the fault area.

1. INTRODUCTION

Efficient earthquake strong-motion array layout for source inversion is investigated by estimating the accuracy of the inversion solution using the array theoretical seismograms. The main purposes are to develop a general rule of strong-motion array layout for source inversion and to provide a reasonable guideline for future planning installations of strong-motion arrays. The effective deployment of strong-motion arrays will lead to remarkable success in estimating high-frequency ground motions in the future, which largely contribute to the reasonable selection of design earthquake motions for critical structures.

At the 1978 International Workshop on Strong Motion Earthquake Instrument Arrays, the first proposal for a desirable array configuration was made on the basis of an empirical judgement for each of three typical types of earthquake faults: a strike-slip fault, a dip-slip fault, and an offshore subduction thrust fault (Ref. 1), and subsequently the importance of dense strong-motion arrays for understanding the nature of high-frequency ground motions has been widely recognized. Up to date, however, no quantitative analysis has yet been done as to how the array stations should be deployed. The deployment strategy of the array stations is undoubtedly required to better understand the limitations on current source inversion studies and to maximize the usefulness of the data which will be obtained.

2. METHODS

The estimation of array layout is performed by using our source inversion method (Ref. 2) developed based on the Wolberg's prediction analysis (Ref. 3). We estimate the accuracy of the solution of waveform source inversion from errors in the data by using the principle of the error propagations. This is done by solving normal equations only once without practically carrying out an inversion procedure for determining fault parameters.

Most of the current source inversion studies deal with a detailed history of rupturing on a fault. We divide the entire fault into many subfaults and use the far-field approximation for the displacement waveform representation at each subfault. Only the far-field S waves in a semi-infinite elastic space are taken into account.

A common, simple source time function which depends upon the subfault size is assumed for each subfault. The seismic moment and the rupture onset time for each subfault are chosen as the unknown parameters. The unknown parameters are determined using a least-squares criterion. Here, uncertainties are assumed for several independent variables. We estimate the accuracy of source inversion, σ , by the maximum standard deviation of errors in estimating the seismic moment for each subfault. It is because errors in estimating the rupture onset time are considerably underestimated since the ground motions are a nonlinear function of the rupture onset time.

In our method, we treat the problem as an overdetermined least-squares problem rather than an underdetermined inverse problem. No attempt is made to stabilize solutions. Instead, we require the 'perfect' resolution of the solution, i.e., the resolution matrix is an identity matrix. Therefore, we use 'variance' as a sole parameter to estimate the accuracy of the inversion. The optimal solution in our method indicates the solution with the minimum variance. The subfault size is important because it gives the 'resolution'.

3. SYSTEMATIC ANALYSIS

A systematic analysis is done to investigate relationships between strong-motion, fault-array parameters and the accuracy of source inversion (Ref. 4). Several fault-array parameters, which are all normalized in this analysis to make the obtained results applicable to a general case, are separately varied and their effects on the accuracy of the source inversion are estimated. In the present paper, the effects of three parameters, i.e., the number of subfaults, N_e , the number of stations, N_s , and the array radius, R , are examined. The fault geometry and the array stations used in this section are shown in Fig. 1. The array stations are distributed at equal intervals in a circle around a strike or dip-slip fault.

We find that normalized uncertainty, σ is roughly proportional to N_e^2 in Fig. 2(a). It should be noted that so good accuracy for a strike-slip fault cannot be expected as for a dip-slip fault. Fig. 2(b) shows that the uncertainty, σ is roughly inversely proportional to the number of stations, N_s . Hence, a relationship of $\sigma \propto N_e^2/N_s$ suggests that numerous stations are required to investigate the detailed fault rupturing process. Also, as shown in Fig. 2(c), the most appropriate is an array which surrounds the fault area sufficiently in its vicinity. The small dependency of the uncertainty on the array radius in the case of a dip-slip event implies that distant stations are as almost effective as near-source stations for a dip-slip fault.

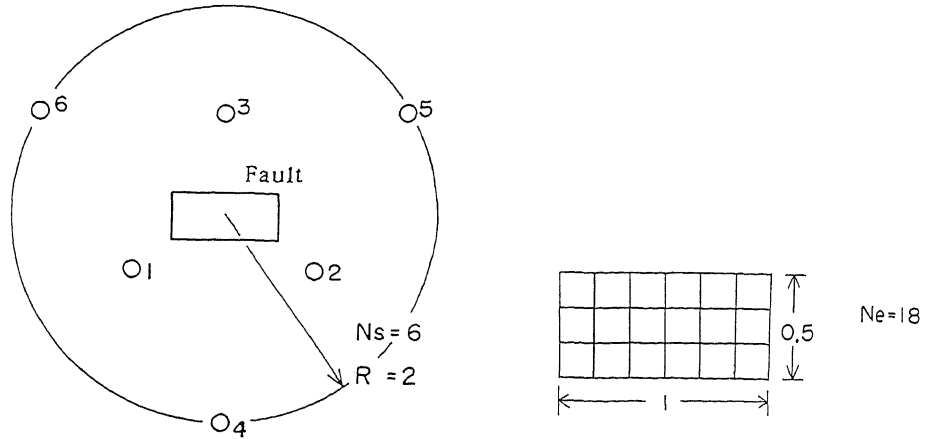


Fig. 1 Geometrical arrangement of faults and array stations. Two kinds of faults are assumed at the center of the array: a pure strike-slip fault with the dip angle, $\delta = 90^\circ$ and a pure dip-slip fault with $\delta = 30^\circ$. All the distances are normalized by the fault length.

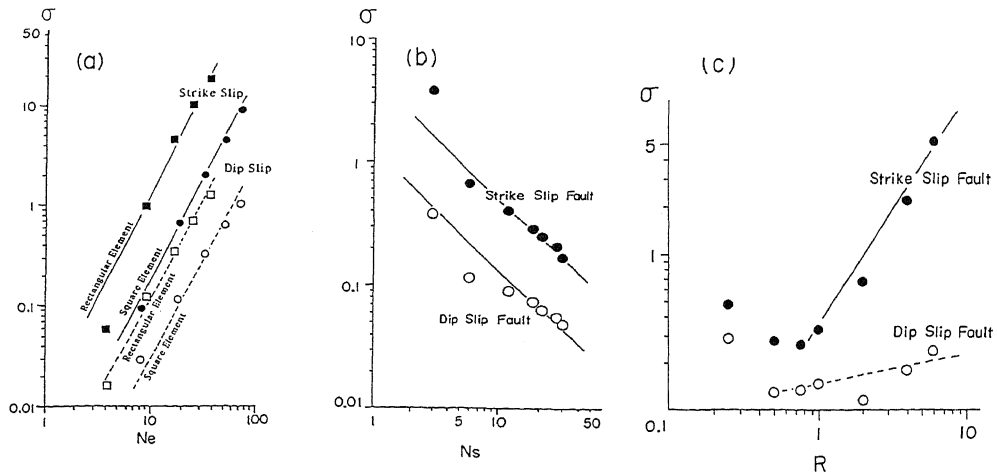


Fig. 2 Relationships between inversion uncertainty, σ and fault-array parameters (the number of subfaults, N_e , the number of stations, N_s , and the array radius, R).

4. OPTIMUM ARRAY GEOMETRY

The optimum array geometry is quantitatively determined by a trial and error modeling for each of three typical types of earthquake faults: a strike-slip fault, a dip-slip fault, and a subduction thrust fault (Ref. 5). By 'optimum', we mean that the solution of source inversion becomes the most accurate with the same number of array stations and for the same process of fault rupturing. In the present paper, the optimum array geometry for a strike-slip fault is determined. By fixing the number of array stations at 16, a wide variety of array configurations are tested (Fig. 3).

The accuracy of source inversion obtained for each array configuration is shown in Fig. 3. We should note that the preferable arrays involve both the near-source stations and the stations encircling the fault area. We find that the former stations resolve the later stage of rupturing process while the latter stations resolve the earlier stage. According to our interpretation, the former stations are sensitive to the perturbations of subfault seismic moments, while the latter stations contribute to the discrimination of the seismic wave radiated from each subfault in the time domain. The optimum array obtained here is rather different from the Workshop one.

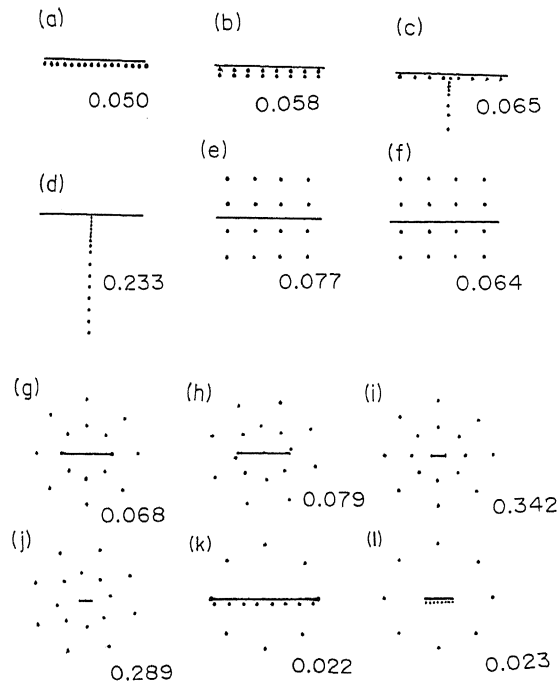


Fig. 3 Various array configurations (map views) tested for a determination of the optimum configuration for a strike-slip fault. The horizontal bar shows the fault and the dots indicate stations. The numerical value indicates the inversion uncertainty obtained.

5. APPLICATION TO EXISTING NETWORKS

Our inversion method is applied to existing strong-motion array networks. Insight into the resolving power of the whole array and the contribution of individual array station is obtained (Ref. 6). In the present paper, the fault rupturing history of the 1979 Imperial Valley earthquake is studied. Two fault models with different resolutions in the distribution of dislocation are used. In the first case, the entire fault is divided into 20 5km x 5km subfaults and in the second case, into 48 3km x 3km subfaults. Three arrays tested are: 13 stations that form the El Centro array (indicated by solid squares), 20 stations located within the United States (solid and open squares), and all 26 stations including 6 Mexican stations (Fig. 4).

The results are summarized in Table 1. The shadowed portion shown in Fig. 4 means the subfault with the largest uncertainty. We should note that the subfault size is largely responsible for the striking variance in the inversion uncertainty. Besides, El Centro array case is a clear indication that stations perpendicular to the fault strike are obviously impertinent to source inversion. The use of Mexican stations contributes to the improvement of the inversion uncertainty due to the good azimuthal coverage.

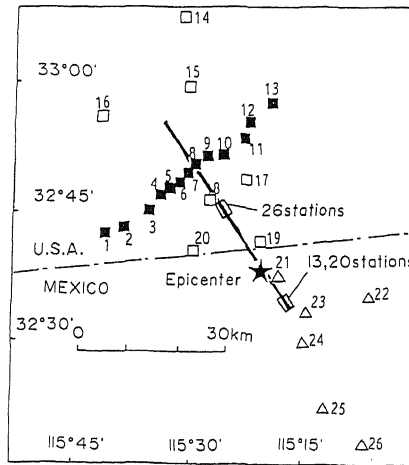


Fig. 4 Local map of the Imperial Valley section of the San Andreas fault showing the fault trace of the 1979 Imperial Valley earthquake and the locations of strong-motion stations. The subfault with the largest inversion uncertainty determined for the case of 48 subfaults is indicated by the shadowed portion.

Table 1 The maximum standard deviation of errors in estimating subfault seismic moments, which is normalized by the seismic moment. N_e is the number of subfaults, N_s is the number of stations, and the numerical value inside the parenthesis is the subfault area.

$N_e \setminus N_s$	13	20	26
20 (5x 5km ²)	1.16	0.25	0.08
48 (3x 3km ²)	40.94	2.79	0.73

6. CONCLUSIONS

A first analysis for estimating the accuracy of the source inversion solution using strong-motion array theoretical seismograms has been carried out in order to develop a general rule of strong-motion array layout for source inversion. For this purpose, a source inversion method has been developed on the basis of the Wolberg's prediction analysis. It has allowed us a systematic analysis to reveal the effects of fault-array parameters. The representative relationship is $\sigma = c \cdot N_e^2 / N_s$, where σ is the accuracy of source inversion, N_e is the number of subfaults, N_s is the number of stations, and c is a constant. It suggests that numerous stations are necessary to infer a detailed fault rupturing process. Also, it has been found that two different kinds of stations must be simultaneously provided regardless of the target fault type. One is composed of stations which surround the fault area with good azimuthal coverage, and the other is composed of near-source stations.

ACKNOWLEDGEMENTS

We wish to thank Profs. Y.Osawa, M.Hakuno, E.Shima, and Dr. K.Kudo at the Earthquake Research Institute, the University of Tokyo, Prof. T.Mikumo at the Disaster Prevention Research Institute, Kyoto University, and Dr. P.Spudich at U.S. Geological Survey for their helpful advice and encouragements. We also want to thank the members of the Seminar of Seismic Activity Group at our research institute (sponsored by Prof. T.Utsu) for helpful discussions.

REFERENCES

1. Iwan,W.D. (Editor), "Strong-Motion Earthquake Instrument Array", Proc. Internatl. Workshop on Strong-Motion Earthquake Instrument Arrays, Honolulu, Hawaii, (1978).
2. Miyatake,T., Iida,M., and Shimazaki,K., "The effect of Strong-Motion Array Configuration on Source Inversion", Bull. Seism. Soc. Am., 76, 1173-1185, (1986).
3. Wolberg,J.R., "Prediction Analysis", D. Van Nostrand Co., Inc., Princeton, New Jersey, (1967).
4. Iida,M., Miyatake,T., and Shimazaki,K., "Relationship between Strong-Motion, Fault-Array Parameters and the Accuracy of Source Inversion", Bull. Seism. Soc. Am., (submitted for publication).
5. Iida,M., Miyatake,T., and Shimazaki,K., "Optimum Strong-Motion Array Geometry for Source Inversion", Earthq. Eng. Struct. Dyn., (submitted for publication).
6. Iida,M., Miyatake,T., and Shimazaki,K., "Preliminary Analysis of Resolving Power of Existing Strong-Motion Arrays for Source Inversion", Bull. Seism. Soc. Am., (submitted for publication).